Korean J. Chem. Eng., **27**(4), 1109-1116 (2010)
DOI: 10.1007/s11814-010-0169-8

Parameter effect on photocatalytic degradation of phenol using TiO_2-P25/activated carbon (AC)

Sze-Mun Lam, Jin-Chung Sin, and Abdul Rahman Mohamed†

School of Chemical Engineering, Universiti Sains Malaysia, Engineering Campus, 14300 Nibong Tebal, Pulau Pinang, Malaysia
(*Received 14 September 2009 • accepted 29 October 2009*)

Abstract−P25 powder embedded and TiO_2 immobilized on activated carbon (TiO_2-P25/AC) was prepared by P25 powder modified sol-gel and dip-coated method. The photocatalysts were characterized by XRD, BET, SEM and their photocatalytic activities were evaluated through phenol degradation in a fluidized bed photoreactor. The addition of P25 in the photocatalysts could significantly enhance the photocatalytic activity, and the optimum loading of P25 was 3 g L^{-1}. The operating parameter results indicated that the optimum pH for phenol degradation was 5.2; the effect of air flow rate gave an optimal value of 2 L min^{-1}; the increasing of UV light intensity led to an increase of degradation efficiency due to more photons absorbed on the surface of the photocatalyst. The kinetics of the phenol degradation fitted well with the Langmuir-Hinshelwood kinetics model. Finally, the photocatalytic ability of TiO_2-P25/AC was reduced only 10% after five cycles for phenol degradation.

Key words: TiO_2-P25/AC, Phenol, Modified Sol-gel, Photocatalytic Degradation, Langmuir-Hinshelwood Model

INTRODUCTION

Phenol and its derivatives are some of the most refractory pollutants present in industrial wastewater such as in the petrochemical, chemical, pharmaceutical, pesticide, plastic and paper industries. Owing to their high toxicity and recalcitrant nature, they are the main reasons why these pollutants not readily degradable [1]. The conventional treatment methods such as biological oxidation, chemical and physical-chemical treatments often have little degradation effect on this kind of pollutant. On the contrary, heterogeneous photocatalysis utilizing TiO_2 have been proven to be effective for them. TiO_2 is an inexpensive, non-toxic and biocompatible material that shows high photoefficiency and activity. Recent reports indicate that simultaneous removal of numerous toxic organic pollutants in water and air can be realized in TiO_2-based photocatalytic reaction systems [2-7]. Thus, it is undoubtedly of great interest that this method can be applied on a large scale for water and wastewater treatment.

However, the application of fine TiO_2 powder is generally accompanied by complications arising from the need for separation of the powder from the treated pollutants, which hinders their wide-scale application in industry. Several efforts have been made to enhance the separation performance of TiO_2 powder, such as immobilization of TiO_2 powder onto various supports [8-11]. Nevertheless, simple coating methods exhibit relatively low photocatalytic activity because of their low TiO_2 dispersion and its contact with light, as well as introducing a possible mass transfer limitation between the treated pollutant and photocatalyst [12-14]. Escape of TiO_2 particle from the supports has also been observed after a period of usage and not suitable for recycling. Recently, several authors have employed commercial TiO_2 powder (Degussa P25) embedded into titanium precursor sol to form composite film to both maintain dispersion and stable film because of their high purity, availability and relatively low cost [15-18]. Moreover, titanium precursor sol could act as a binder (matrix) around Degussa P25 to immobilize P25 particles on the supports. The advantage of using this technique for the preparation of TiO_2 films is that the high purity Degussa P25 powder can be well immobilized by the presence of sol-gel derived TiO_2 matrix [7].

So far, attempts to immobilize these composite films on supports including glass beads, glass and stainless steels have been developed for the photocatalytic degradation of organic pollutants [7,13,16, 18,19]. However, the activity for the degradation of organic pollutants by other sorbents as supporter of photocatalyst still remains unreported. These sorbents often used include silica gels, activated carbon, zeolites, and clays. The sorbents are so selected that they can be easily suspended by air bubbling or mechanical stirring. Among these sorbents, activated carbon (AC) is an excellent alternative because of its high adsorption capacity and high specific area. Furthermore, adding TiO_2 to AC could induce some beneficial effect because of the highly adsorptive characteristic of AC with respect to organic molecules and also resolve the problem of achieving optimum adsorption strength of the adsorbed molecules on the adsorbent to improve TiO_2 photocatalytic activity [20]. In fact, some authors have also reported a synergistic effect for AC-supported TiO_2 systems of some organic pollutants in the photocatalytic process [21-24].

In the present work, TiO_2-P25/AC photocatalyst was prepared by the P25 powder modified sol-gel and dip-coated method. Their photocatalytic activities were evaluated by degradation of phenol in a fluidized bed photoreactor. The effects of operating parameters on the photocatalytic activity of TiO_2-P25/AC were investigated and the kinetics of phenol degradation was also analyzed. In addition, a recycling test was performed to examine the repeatability of the photocatalyst.

†To whom correspondence should be addressed.
E-mail: chrahman@eng.usm.my

EXPERIMENTAL

1. Preparation of TiO_2-P25/AC

The TiO_2-P25/AC was prepared by the P25 powder modified sol-gel and dip-coated method. The procedure for the preparation of P25 powder modified sol-gel was described by Balasubramanian et al. [13]. Then, 2.0 g of AC with a particle size of 1.18-2.36 mm, pre-washed with deionized water was added in the modified sol-gel. After mixing and stabilization for 30 min, the photocatalysts were dried at 60 °C for 12 h in an oven. Subsequently, the photocatalysts were subjected to heat treatment in a multi-segment programmable high temperature furnace. The furnace temperature was incremented at a ramp rate of 3.0 °C min^{-1} until 100 °C, where it was held for 1 h. After that, the temperature was increased at a ramp rate of 3.0 °C min^{-1} to the final temperature (400, 500, 600 and 700 °C) and held for another 1 h. Finally, the photocatalyst was cooled to 35 °C at a rate of 5 °C min^{-1}. All obtained TiO_2-P25/AC photocatalysts were dip-coated twice.

2. Photocatalytic Degradation Experiment

The photocatalytic degradation of phenol solution was carried out in a fluidized bed photoreactor (shown in Fig. 1). The photoreactor was equipped with a quartz column of 600 mm height, 60 mm external diameter and with a wall 0.5 mm thick that was used as the main chamber for the photocatalytic processes. The phenol solutions were illuminated by four 20 W germicidal UV lights (254 nm, Sankyo Denki Co. Ltd.) placed around the quartz column to provide illumination for photocatalytic reaction. The intensity for each UV light inside the quartz column at distance 55 mm away from UV light, measured by radiometer (Cole Parmer, Series 9811) was in the range of 210 to 236 μW cm^{-2}. The total UV intensity was 921 μW cm^{-2} by turning on all the UV lights. 1,400 mL of phenol solution with the concentration (25 mg L^{-1} to 130 mg L^{-1}) and about 2.58 g TiO_2-P25/AC (TiO_2-P25 concentration of 0.41 g L^{-1}) were fed into the photoreactor column. The solution pH (2.0-12.0) was adjusted by adding small amount of 1.0 M HCl or NaOH to the desired value throughout the experiments. To maintain a fluidized condition, the air flow rate was adjusted to (0.5 L min^{-1} to 3 L min^{-1}) by rotameter (model 32464-12 from Cole-Parmer) and aerated from the bottom through an air distributor. A mesh (size of 200 μm) was used with the air distributor to provide a uniform fluidization of the photocatalyst. A thermocouple was placed inside the quartz glass column of the fluidized bed photoreactor to monitor the temperature changes during the photocatalytic experiments. All experiments were conducted in batch mode and reaction temperature of 30 °C.

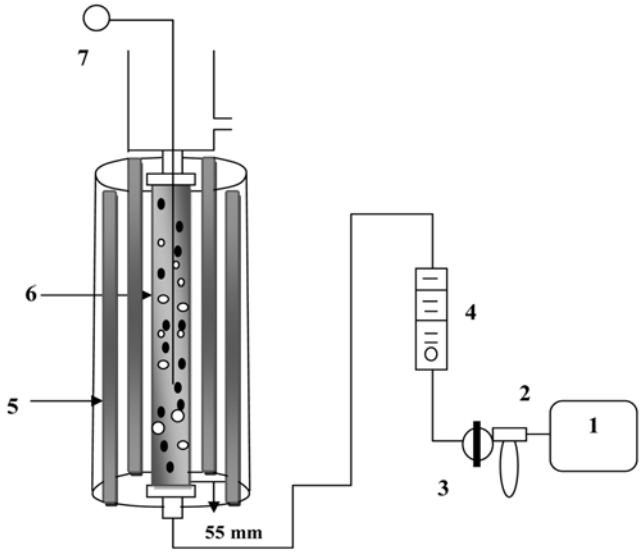

Fig. 1. Fluidized bed photoreactor. (1) Air compressor; (2) air filter; (3) pressure gauge; (4) rotameter; (5) UV light; (6) photocatalytic reaction column and (7) thermocouple.

3. Analytical Methods

At the given irradiation time intervals, the phenol solutions were sampled. The collected samples were then filtered through a 0.45 μm PTFE syringe filter prior to analysis for separation of the any suspended solid. The clean transparent solution was analyzed by high performance liquid chromatography (HPLC, Perkin Elmer Series 200) equipped with an isocratic gradient pump, a 20 μL injection circuit and a variable wavelength UV detector. *C18* column (150 mm-length×4.6 mm-ID×5 μm-particle size) was used in the sample analysis with a mobile phase mixture of water 60% (v/v) and acetonitrile 40% (v/v) at a flow rate of 1 mL min^{-1}. The wavelength of the detector was set at 238 nm.

The prepared samples were characterized by measuring Brunauer-Emmett-Teller (BET) surface area by nitrogen adsorption (Micromeritics ASAP 2020). Single point surface area was measured at P/P_o= 0.3, and single point total pore volume of pores less than 67 nm diameter at P/P_o=0.97. X-ray diffraction (XRD) measurements of samples were carried out using a diffractometer PW 1820 system (Philips) with Cu Kα irradiation (λ=0.15418 nm). The accelerating voltage of 40 kV and an emission current of 30 mA at an angle of 2θ from 20° to 70° were used. The surface morphology of prepared catalysts was observed by scanning electron microscopy (SEM) 50VP Field Emission (Leo Supra) at a voltage of 20 kV.

RESULTS AND DISCUSSION

1. Effect of Calcination Temperature on TiO_2-P25/AC

According to literature reports, the photocatalytic activity of TiO_2

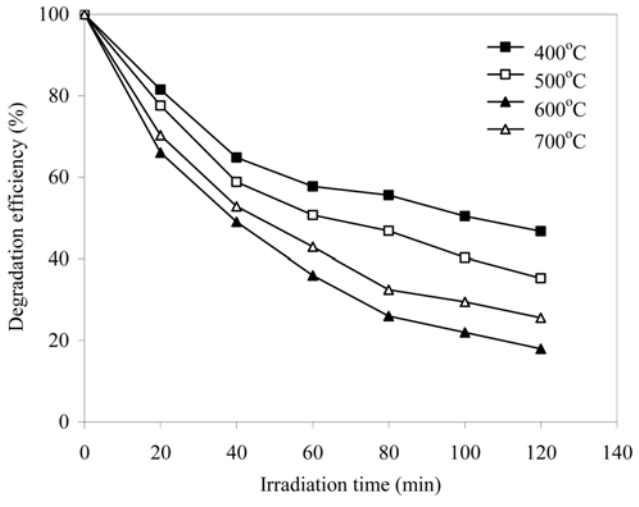

Fig. 2. Effect of calcination temperature on the photocatalytic degradation of phenol ([phenol]=50 mg L^{-1}; UV light intensity=921 μW cm^{-2}; air flow rate: 2 L min^{-1}; pH=5.2; [TiO_2-P25]=0.36 g L^{-1}).

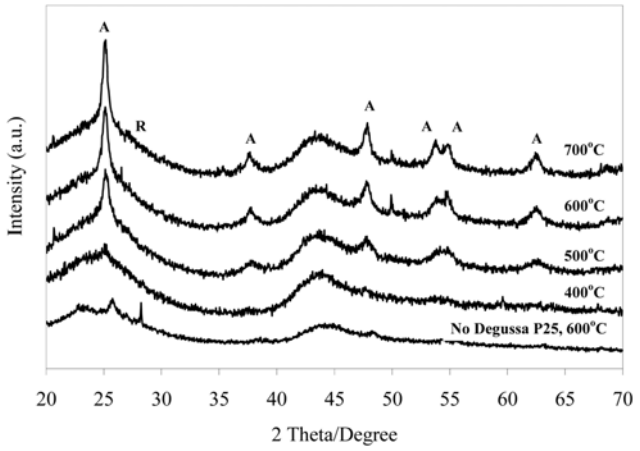

Fig. 3. XRD patterns of the 1 g L^{-1} P25 powder in TiO_2-P25/AC prepared at different calcination temperatures (A: anatase; R: rutile).

is greatly affected by the calcination temperature [17,25,26]. To obtain the optimal calcination temperature for TiO_2-P25/AC preparation, the photocatalysts were calcinated at different temperatures in the range of 400 to 700 °C, for investigating the photocatalytic degradation of phenol. The results are presented in Fig. 2. As can be seen, the calcination temperatures significantly influence the photocatalytic activity of TiO_2-P25/AC and the optimum calcination temperature was 600 °C. In addition, X-ray diffraction was used to determine the crystalline structure and phase of the catalysts. Fig. 3 shows the XRD patterns for TiO_2-P25/AC prepared at different calcination temperatures. It can be observed that the TiO_2-P25/AC calcinated at 600 °C revealed both anatase and rutile phases of TiO_2, which can explain the higher photocatalytic activity for the degradation of phenol. Recent reports on the mixture of anatase and rutile phase photocatalyst have shown higher photocatalytic activity [13,27,28]. This could be attributed to the fact that the presence of rutile phase enhances the anatase phase by serving as an electron sink. By capturing the photogenerated electrons from the anatase crystals, the rutile phase stabilizes the holes generated in the anatase phase by preventing recombination. Therefore, more holes are available in the anatase phase for reaction with hydroxyl ion to form hydroxyl radicals (•OH). From the XRD patterns, the rutile phase was not clearly seen in the TiO_2-P25/AC. The reason could be that (i) the anatase to rutile transformation is usually expected to take place between 700 °C and 800 °C [28], (ii) the P25 loading in the photocatalyst is low, and (iii) the ratio of rutile phase in Degussa P25 is relatively low (15-30% rutile phase). Hence, it is reasonable to conclude that such a low rutile composition in the TiO_2-P25/AC photocatalysts was too small to be seen in the patterns. The crystalline particle size of the photocatalyst was determined from the Scherrer formula, and the particle sizes of TiO_2 were in the range of 7 to 19 nm as shown in Table 1.

Table 1. The crystallite size (D), BET surface area (S_{BET}) and total pore volume (V_{tot}) of 1 g L^{-1} P25 powder in TiO_2-P25/AC photocatalysts prepared at different calcination temperatures (T_c)

Catalyst	T_c (°C)	D (nm)	S_{BET} (m^2 g^{-1})	V_{tot} (cm^3 g^{-1})
TiO_2-P25/AC	400	7	815	0.4409
	500	7.5	809	0.4317
	600	10	788	0.4261
	700	19	613	0.3450

The BET method was used to determine the surface area and total pore volume of the photocatalysts. Table 1 also shows the BET data for TiO_2-P25/AC prepared at different calcination temperatures. The results revealed that the BET surface area of photocatalyst prepared at calcination temperature from 400 to 600 °C did not decrease obviously. Higher calcination temperature caused rapid decrease of BET surface area for photocatalyst prepared at 700 °C, possibly due to crystallites agglomerating into bigger crystal particles. There was a similar change in the total pore volume. Considering the crystallization, surface area and total pore volume characteristics, the optimal calcination temperature was 600 °C and was used for all the following experiments.

2. Optimum Loading of P25

To evaluate the effect of the addition of P25 loading on the photocatalytic activity of TiO_2-P25/AC, a series of experiments were performed with different embedded loadings of P25 from 0 to 6 g L^{-1}. Fig. 4 presents the effect of P25 loading on the photocatalytic degradation of phenol. The results demonstrated that the addition of P25 loading could enhance the photocatalytic activity of TiO_2 film. In addition, all the TiO_2-P25/AC had higher photocatalytic activity than pure TiO_2/AC. At the optimum P25 loading of 3 g L^{-1}, the TiO_2-P25/AC showed the highest photocatalytic activity.

The enhancement of photocatalytic activity could be ascribed to several reasons. On the one hand, in the course of phenol photocatalytic degradation by pure TiO_2/AC, the amounts of crystalline materials were relatively low because only crystalline formed from the alkoxide sol-gel (shown in Fig. 3). The addition of P25 loading in the TiO_2-P25/AC was composed of P25 particles together in the presence of crystallites from alkoxide sol-gel which hence increased the interface area between the TiO_2-P25 particles and phenol molecules. In addition, TiO_2-P25/AC calcinated at 600 °C is advanta-

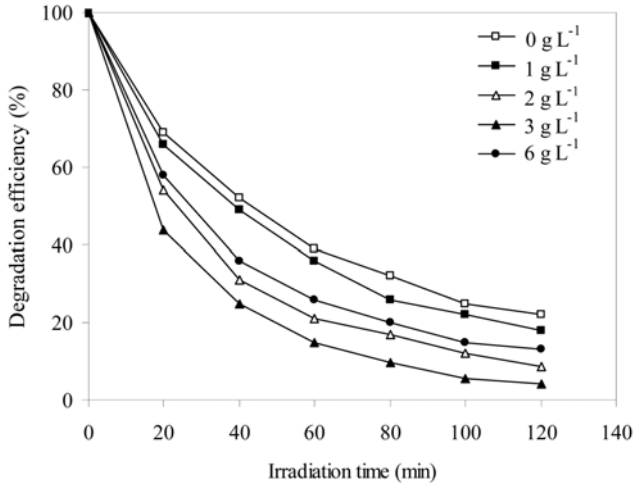

Fig. 4. Effect of P25 loading on the photocatalytic degradation of phenol ([phenol]=50 mg L^{-1}; UV light intensity=921 μW cm^{-2}; air flow rate: 2 L min^{-1}; pH= 5.2; [TiO_2-P25]=0.41 g L^{-1}).

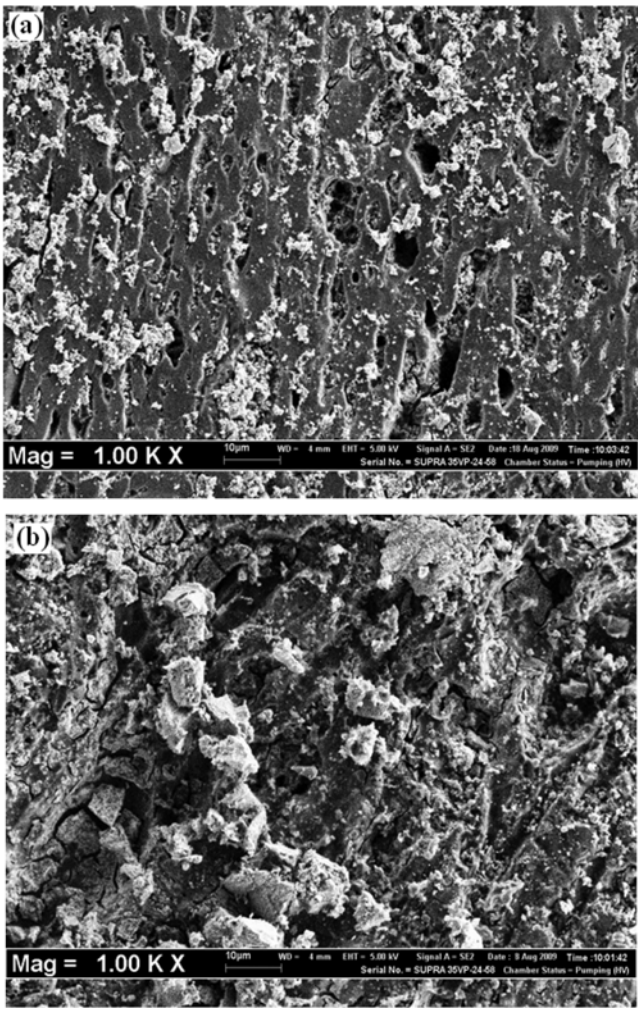

Fig. 5. SEM images of the TiO_2-P25/AC prepared at (a) 3 g L^{-1} P25 powder and (b) 6 g L^{-1} P25 powder.

geous because it consists of anatase and rutile phases, and this catalyst has much larger surface area, which in turn could have a beneficial effect on the photocatalytic activity. However, the excessive loading of P25 in the photocatalyst can tend to increase the number of agglomerates in the TiO_2 film and result in lower photocatalytic activity. Furthermore, scanning electron microscopy was employed to examine the surface morphology of the photocatalysts. Fig. 5(a) and (b) show the SEM images of TiO_2-P25/AC photocatalysts prepared with 3 g L^{-1} and 6 g L^{-1} of P25 loading, respectively. It was found that the agglomerates of TiO_2-P25 particles were well immobilized on AC support. Moreover, the SEM images show that the surface area covered by these agglomerates increased with an increase in the P25 loading from 3 to 6 g L^{-1} in the photocatalyst. Therefore, 3 g L^{-1} was the optimal P25 loading in the TiO_2-P25/AC for the photocatalytic activity enhanced by increasing the exposure area of solid-liquid interface.

3. Effect of Solution pH

The solution pH exhibits profound influence on TiO_2 surface charge and adsorption ability [26]. Therefore, the role of pH on the photocatalytic degradation of phenol was studied in the pH range of 2.0 to 12.0. The results are presented in Fig. 6. It can be seen that the

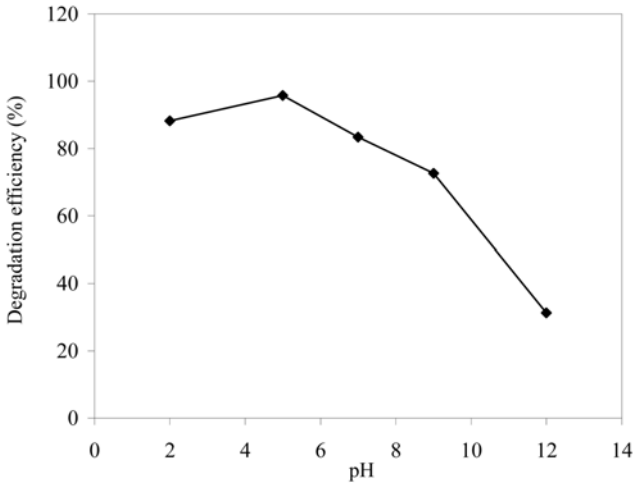

Fig. 6. Effect of solution pH on the photocatalytic degradation of phenol ([phenol]=50 mg L^{-1}; UV light intensity=921 μW cm^{-2}; air flow rate: 2 L min^{-1}; [TiO_2-P25]=0.41 g L^{-1}).

degradation efficiency of phenol increased when the solution pH increased from pH 2.0 to 5.2 (natural pH). However, a further increase in the solution pH, led to a decrease in the degradation efficiency of phenol. The results indicated that the optimal solution pH for photocatalytic degradation of phenol was observed at pH of 5.2, which was also similar to that reported by other authors [14,26,29].

According to the point of zero charge (pH_{pzc} 6.25) of TiO_2 [30], the following surface reactions are expected to occur at different pH values (Eq. (1) and (2)):

$$pH<pH_{pzc}: TiOH+H^+ \rightarrow TiOH_2^+ \quad (1)$$

$$pH>pH_{pzc}: TiOH+OH^- \rightarrow TiO^-+H_2O \quad (2)$$

where TiOH is the surface 'titanol' group. Thus, it is reasonable to expect that the electrical charge of the phenol and the catalyst surface will determine the extent of adsorption. At a low pH, phenol was primarily in its molecular form and the surface of TiO_2 was positively charged. For pH 2.0, the pH was adjusted by HCl, while the Cl^- anions might have been adsorbed on the surface of TiO_2 [31-33]. This has been proved by Chen and Ray [31] that a competition between the adsorption of the Cl^- anions and phenol would happen on the TiO_2 surface to decrease the photocatalytic activity. However, at the pH 5.2, the Cl^- anions did not exist because the natural pH did not require the addition of any HCl to adjust the pH solution. Consequently, the electrostatic attraction between positively charged TiO_2 with phenol molecules resulted in maximum adsorption, and thus led to high degradation efficiency of phenol.

On the other hand, at higher pH, as phenol molecules are negatively charged in alkaline media, their adsorption is also expected to be affected by an increase in the density of TiO^- groups on the catalyst surface. Thus, due to Coulombic repulsion the phenols are scarcely adsorbed [30]. Besides, the pH was adjusted by NaOH for higher pH value. Bekkouche et al. [33] had reported that the adsorption of the Na^+ ions and OH^- ions could create a competition with the phenolate anions on the surface of TiO_2, also resulting in lower photocatalytic activity. For the above reasons, the photocatalytic activity of phenol reached a maximum in slight acidic condi-

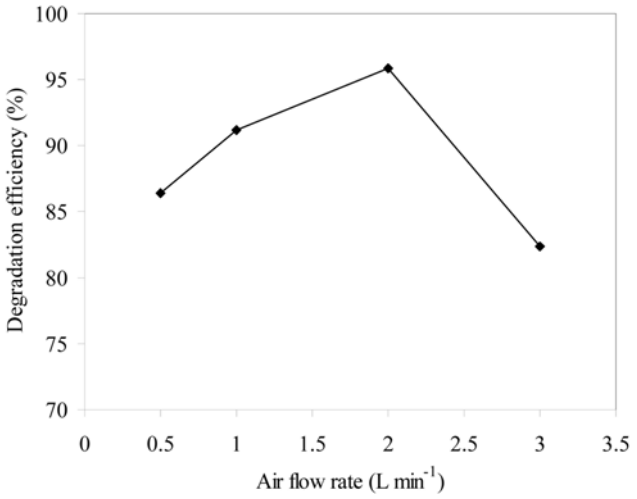

Fig. 7. Effect of air flow rate on the photocatalytic degradation of phenol ([phenol]=50 mg L^{-1}; UV light intensity=921 μW cm^{-2}; [TiO_2-P25]=0.41 g L^{-1}; pH= 5.2).

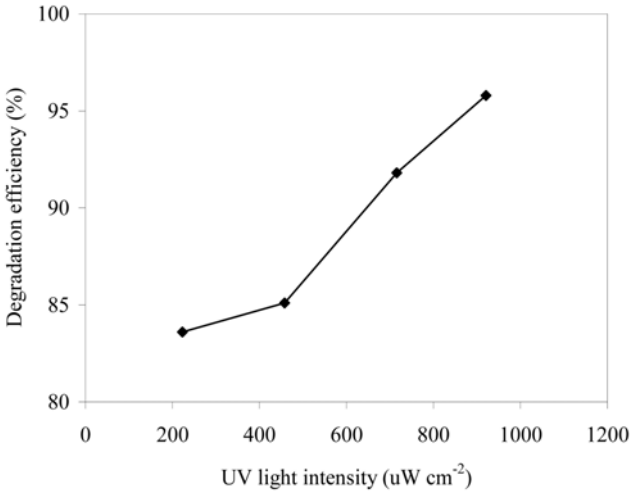

Fig. 8. Effect of UV light intensity on the photocatalytic degradation of phenol ([phenol]=50 mg L^{-1}; air flow rate=2 L min^{-1}; [TiO_2-P25]=0.41 g L^{-1}; pH=5.2).

tions (pH 5.2) and followed by a decrease in the pH range 7.0 to 12.0.

4. Effect of Air Flow Rate

Since the fluidized bed photoreactor used is operated as an immobilized type reactor, the total delivered air flow rate was significant for this study. Compressed air was used as the air flow sources to not only maintain adequate suspension and better mixing condition, but also provide sufficient amount of dissolved oxygen. In this study, different air flow rates varying from 0.5 to 3.0 L min^{-1} were investigated. The effect of air flow rate on the photocatalytic degradation of phenol is illustrated in Fig. 7. It can be seen that the degradation of phenol increased with increasing air flow rate up to the limit 2.0 L min^{-1}; beyond this limit, there was a decrease in the degradation efficiency. Similar observations have been reported concerning the photocatalytic degradation of other pollutants [34-36].

The influence of air flow rate on the photocatalytic degradation of phenol can be explained in terms of the turbulence induced by the air bubbles and oxygen supply for photocatalytic reaction [36,37]. As the rate of air flow was increased, an increase in the turbulence induced by the air bubbles was observed. Thus, the probability of photocatalyst contacting with phenol molecules increased and resulted in a higher mass transfer rate. However, at the higher air flow rate (over the optimal air flow rate), the fluidized bed was expanded due to the creation of larger air bubbles, which may hinder the absorbance of UV light to the photocatalyst. Therefore, it can be said that there is an optimal air flow rate for the fluidized bed photoreactor.

In addition, the concentrations of dissolved oxygen in the phenol solution after passing through the fluidized bed photoreactor were also measured by means of dissolved oxygen meter. The actual dissolved oxygen was found to be 7.7-8.0 mg L^{-1} at the air flow rate of 2 L min^{-1}. Several authors have also demonstrated that there existed a sufficient amount of dissolved O_2 when optimal air flow rate was used in their photocatalytic degradation system [38-41]. The role of dissolved O_2 is to enhance the separation of the photogenerated electrons and holes and thereby improve the efficiency with which the •OH radicals are produced. Therefore, in this study, 2.0 L min^{-1} was the optimum air flow rate for the fluidization of photocatalysts enhancing the photocatalytic reaction by increasing the mass transfer and by scavenging the photogenerated electrons.

5. Effect of UV Light Intensity

The effect of UV light intensity on the photocatalytic degradation of phenol was studied by using 1, 2, 3 and 4 UV lights corresponding to the light intensity of 223, 458, 716 and 921 μW cm^{-2}, respectively as measured by radiometer. Fig. 8 shows the phenol concentration as a function of irradiation time under four different UV light intensities. As UV light intensity increased from 223 to 921 μW cm^{-2}, the degradation efficiency of phenol increased linearly and reached the maximum when the UV light intensity was 921 μW cm^{-2}. Apparently, the UV light intensity has a positive effect on the degradation efficiency of phenol.

UV light intensity determines the amount of photons absorbed by the photocatalyst. With the increase of the UV light intensity, the photocatalyst absorbs more photons, producing more electron-hole pairs in the photocatalyst surface and this increases the •OH radical concentration and consequently increases the degradation efficiency. Earlier studies [42,43] on the effect of the UV light intensity have stated that at low light intensity (catalyst dependent, surface reaction limited) the rate is linearly proportional to the light intensity, while at medium-high intensity, the rate becomes proportional to the square root of the light intensity, and at higher light intensity, the rate would not be affected by the increase of the light intensity. They have attributed this variation to the recombination of photogenerated electron and hole pairs under different radiation intensities. In the present study, the results revealed that the UV light intensity lay within the linear range, where utilization of light energy is most efficient. The finding was in line with several studies which generally observed an increase in photocatalytic degradation efficiency with UV light intensity [44-46].

6. Effect of Initial Substrate Concentration

The dependency of photocatalytic degradation of phenol on the initial substrate concentration is presented in Fig. 9. The examined range of the initial phenol concentration varied from 25 to 130 mg

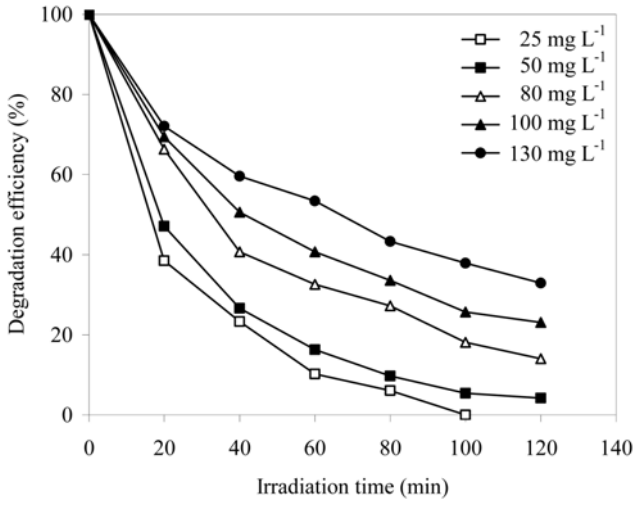

Fig. 9. Effect of initial phenol concentration on the photocatalytic degradation of phenol (UV light intensity=921 μW cm^{-2}; air flow rate=2 L min^{-1}; [TiO_2-P25]=0.41 g L^{-1}; pH=5.2).

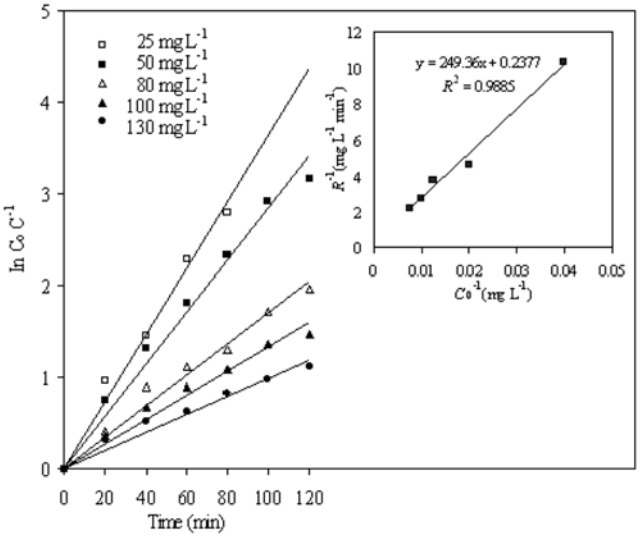

Fig. 10. Kinetics of phenol photocatalytic degradation for different initial phenol concentrations in the presence of 3 g L^{-1} P25 powder in TiO_2-P25/AC. Inset: Linearized reciprocal kinetic plot.

L^{-1}. The results demonstrated that the degradation efficiency of phenol decreased with an increase in the initial concentration of phenol. It was also found that the photocatalytic degradation of phenol obeyed pseudo-first-order kinetics. Fig. 10 exhibits the linear plot of ln (C_0/C) against irradiation time. The apparent rate constants, k_{app} (min^{-1}) were calculated from the slopes of the lines and found to decrease with an increase in the initial phenol concentration as shown in Table 2.

Many authors have demonstrated that the kinetic model for heterogeneous photocatalytic reaction can be described by the Langmuir-Hinshelwood (L-H) kinetic expression [47-49]. The kinetic model assumes that the surface coverage of substrate, which in relation to the concentration in the bulk solution affects the rate of degradation [50]. According to the L-H model, the rate of the photocatalytic degradation of phenol is commonly expressed as Eq. (3):

Table 2. The value of the apparent rate constant (k_{app}) and correlation coefficient (R^2) at different initial phenol concentrations

Initial phenol concentration (mg L^{-1})	k_{app} (min^{-1})	R^2
25	0.0365	0.9846
50	0.0284	0.9816
80	0.0171	0.9750
100	0.0134	0.9640
130	0.0100	0.9544

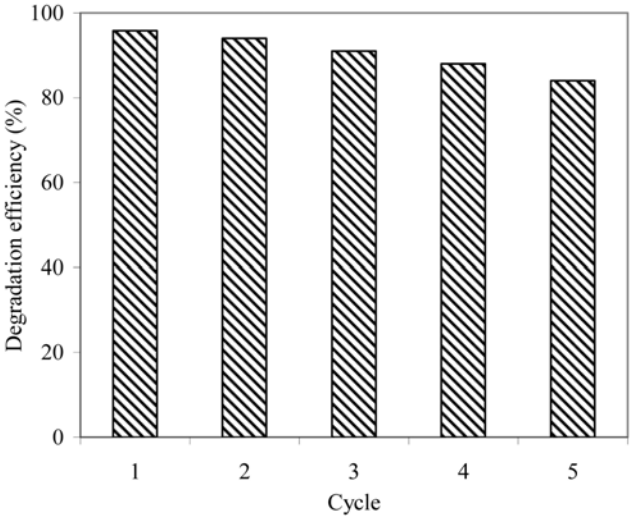

Fig. 11. Degradation efficiency of 3 g L^{-1} P25 powder in TiO_2-P25/AC for phenol photocatalytic degradation of five cycles ([phenol]=50 mg L^{-1}; UV light intensity=921 μW cm^{-2}; air flow rate: 2 L min^{-1}; pH=5.2; [TiO_2-P25]=0.41 g L^{-1}).

$$R = \frac{kKC}{1+KC} = k_{app}C \quad (3)$$

where R is the photocatalytic degradation rate of phenol (mg L^{-1} min^{-1}), C is the initial concentration of phenol (mg L^{-1}), k is the reaction rate constant (mg L^{-1} min^{-1}) and K is the adsorption equilibrium constant (L mg^{-1}). Linearization of Eq. (3) provides the relationship Eq. (4):

$$\frac{1}{R} = \frac{1}{kKC} + \frac{1}{k} \quad (4)$$

By plotting the reciprocal of rate (1/R) against the reciprocal of initial concentration (1/C_0), the validity of the model can be confirmed if the linearization is correct. Moreover, the values of apparent reaction rate constant k and adsorption equilibrium constant K can be determined by linear regression. As shown in Fig. 10 inset, the L-H model can approach correctly the experimental data. This means that the kinetic reaction step is probably the limited step. The obtained values of k and K were 4.206 mg L^{-1} min^{-1} and 0.0010 L mg^{-1}, respectively. These constant values are the same order of magnitude as those reported in the literature for the photocatalytic degradation of other organic pollutants [31,39,47].

The initial substrate concentration dependence of the rate of pho-

tocatalytic degradation of phenol can be realized by the fact that the degradation reaction occurs on TiO_2-P25 particles as well as in solution [51,52]. On the surface of TiO_2-P25 particles, the reaction occurs between the •OH radicals, generated at the active OH^- sites and a phenol molecule from the solution. When the initial concentration is high, the number of these available active sites is reduced by phenol molecules because of their competitive adsorption on TiO_2-P25 particles. Since the intensity of UV light and irradiation time are constant, the •OH radicals formed on the surface of TiO_2-P25 remain practically the same. Thus, the reactive •OH attacking the organic pollutants decreases due to the lower ratio of the •OH/phenol. On the other hand, a significant amount of UV light may be absorbed by the phenol molecules rather than the TiO_2-P25 at higher initial phenol concentration [32,53]. Consequently, the UV light absorbed by the phenol is not effective to carry out the degradation and a decrease in the rate of photocatalytic degradation is observed.

7. Repeatability of Photocatalyst

Recycling use of photocatalyst is very important for the practical application. To evaluate the stability of TiO_2-P25/AC, recycling experiments were performed. For each new cycle, the photocatalyst was filtered, washed and left at room temperature during 24 h. The results are in Fig. 11. After five cycles, the degradation efficiency of phenol reduced only about 10% from 95.8% to 84.0%. The results revealed that the photocatalytic activity of TiO_2-P25/AC photocatalyst has repeatability. Similar results were obtained in TiO_2 immobilized AC system [54]. The reduction in the degradation efficiency among the cycles can be explained by the loss of photocatalyst because of the difficulty to avoid any loss of catalyst materials during the experiments. When investigating the photocatalyst losses before and after five times reuse, the TiO_2-P25/AC mass loss was 4.2 wt%. On the other hand, the TiO_2-P25 immobilized on AC almost did not release or dissolve into the solution, which indicates that photocatalyst was very stable.

CONCLUSION

The present work has studied the TiO_2-P25/AC photocatalyst preparation and photocatalytic degradation of phenol in a fluidized bed photoreactor. The results are summarized as follows:

- The optimum preparation conditions of TiO_2-P25/AC were the calcination temperature 600 °C and the P25 loading of 3 g L^{-1}. XRD patterns revealed that the crystalline phase of TiO_2 in the TiO_2-P25/AC photocatalyst was both anatase and rutile phases. The surface morphology of TiO_2-P25/AC was significantly affected by P25 loading embedded in photocatalyst.
- The optimal solution pH was found to be equal to 5.2.
- A high air flow rate of 3 L min^{-1} has a negative effect on the degradation efficiency due to the creation of larger air bubbles, which may hinder the absorbance of UV light to the photocatalyst.
- On the contrary, the UV light intensity leads to the enhancement of the degradation efficiency because of more photons absorbed on the surface of the photocatalyst.
- The influence of the initial substrate concentration was evaluated and fitted well with the Langmuir-Hinshelwood kinetics model. This allows one to determine the values of the constants' model and to verify its validity.
- Finally, the photocatalytic ability of photocatalyst was reduced only 10% after five cycles for phenol degradation. Owing to its high performance and recycling ability, the TiO_2-P25/AC is a very promising photocatalyst for the degradation of organic pollutants.

ACKNOWLEDGEMENTS

The authors would like to acknowledge the Ministry of Science, Technology and Innovation (MOSTI) under Science Fund Grant (no. 6013338) and Universiti Sains Malaysia Fundamental Research Grant Schemes (FRGS) (no. 811068), which resulted in this article.

REFERENCES

1. C. W. Oh, G. D. Lee, S. S. Park, C. S. Ju and S. S. Hong, *Korean J. Chem. Eng.*, **22**, 547 (2005).
2. A. L. Linsebigler, G. Q. Lu and J. T. Yates, *Chem. Rev.*, **95**, 735 (1995).
3. M. R. Hoffman, S. T. Martin, W. Choi and D. W. Bahnemann, *Chem. Rev.*, **95**, 69 (1995).
4. A. Fujishima, T. N. Rao and D. A. Tryk, *J. Photochem. Photobio. C: Photochem. Rev.*, **1**, 1 (2000).
5 P. R. Gogate and A. B. Pandit, *Adv. Environ. Res.*, **8**, 501 (2004).
6. R. Thiruvenkatachari, S. Vigneswaran and I. S. Moon, *Korean J. Chem. Eng.*, **25**, 64 (2008).
7. Y. J. Chen, E. Stathatos and D. D. Dionysiou, *J. Photochem. Photobio. A: Chem.*, **203**, 192 (2009).
8. V. Durgakumari, M. Subrahmanyam, K. V. Subba Rao, A. Ratnamala, M. Noorjahan and K. Tanaka, *Appl. Catal. A: Gen.*, **234**, 155 (2002).
9. M. Kang, *Appl. Catal. B: Environ.*, **37**, 187 (2002).
10. F. Thevenet, O. Guaitella, J. M. Herrmann, A. Rousseau and C. Guillard, *Appl. Catal. B: Environ.*, **61**, 58 (2005).
11. J. K. Han, S. M. Choi and G. H. Lee, *Mater. Lett.*, **61**, 3798 (2007).
12. X. Z. Li and H. Liu, *Environ. Sci. Tech.*, **37**, 3989 (2003).
13. G. Balasubramanian, D. D. Dionysiou, M. T. Suidan, I. Baudin and J. M. Laine, *Appl. Catal. B: Environ.*, **47**, 73 (2004).
14. S. X. Liu, X. Y. Chen and X. Chen, *J. Hazard. Mater.*, **143**, 257 (2007).
15. G. Balasubramanian, D. D. Dionysiou and M. T. Suidan, *J. Mater. Sci.*, **38**, 823 (2003).
16. M. Keshmiri, M. Mohseni and T. Troczynski, *Appl. Catal. B: Environ.*, **53**, 209 (2004).
17. Y. J. Chen and D. D. Dionysiou, *J. Mol. Catal. A: Chem.*, **244**, 73 (2006).
18. Y. J. Chen and D. D. Dionysiou, *Appl. Catal. A: Gen.*, **317**, 129 (2007).
19. Y. J. Chen and D. D. Dionysiou, *Appl. Catal. B: Environ.*, **69**, 24 (2006).
20. J. Matos, J. Laine and J. M. Herrmann, *Appl. Catal. B: Environ.*, **70**, 461 (2007).
21. D. K. Lee, S. C. Kim, S. J. Kim, I. S. Chun and S. W. Kim, *Chem. Eng. J.*, **102**, 93 (2004).
22. Y. J. Li, X. D. Li, J. W. Li and J. Yin, *Wat. Res.*, **40**, 1119 (2006).
23. Y. J. Li, S. Y. Zhang, Q. M. Yu and W. B. Yin, *Appl. Surf. Sci.*, **253**, 9254 (2007).
24. Y. Z. Liu, S. G. Yang, J. Hong and C. Sun, *J. Hazard. Mater.*, **142**, 208 (2007).

25. C. R. Chenthamarakshan, N. R. D. Tacconi, R. Krishnan and R. Shiratsuchi, *Electrochem. Communications*, **4**, 871 (2002).
26. C. G. Silva and J. L. Faria, *J. Mol. Catal. A: Chem*., **305**, 147 (2009).
27. B. Sun and P. G. Smirniotis, *Catal. Today*, **88**, 49 (2003).
28. J. M. Valtierra, J. G. Servin, C. F. Reyes and S. Calixto, *Appl. Surf. Sci*., **252**, 3600 (2006).
29. K. Naeem and O. Y. Feng, *J. Environ. Sci*., **21**, 527 (2009).
30. C. H. Chiou, C. Y. Wu and R. S. Juang, *Chem. Eng. J*., **139**, 322 (2008).
31. D. W. Chen and A. K. Ray, *Wat. Res*., **32**, 3223 (1998).
32. I. K. Konstantinou and T. A. Albanis, *Appl. Catal. B: Environ*., **49**, 1 (2004).
33. S. Bekkouche, M. Bouhelassa, N. H. Salah and F. Z. Meghlaoui, *Desalination*, **166**, 355 (2004).
34. Y. S. Na, S. K. Song and Y. S. Park, *Korean J. Chem. Eng*., **22**, 196 (2005).
35. T. H. Lim and S. D. Kim, *Chem. Eng. Processing*, **44**, 327 (2005).
36. W. S. Nam, K. C. Woo and G. Y. Han, *J. Ind. Eng. Chem*., **15**, 348 (2009).
37. M. F. J. Dijkstra, A. Michorius, H. Buwalda, H. J. Panneman, J. G. M. Winkelman and A. A. C. M. Beenackers, *Catal. Today*, **66**, 487 (2001).
38. H. Zhu, M. P. Zhang, Z. F. Xia and K. C. Gary Low, *Wat. Res*., **29**, 2681 (1995).
39. W. S. Nam, J. M. Kim and G. Y. Han, *Chemosphere*, **47**, 1019 (2002).
40. L. F. Zhang, T. Kanki, N. Sano and A. Toyoda, *Sep. Purif. Tech*., **31**, 105 (2003).
41. M. N. Chong, B. Jin, H. Y. Zhu, C. W. K. Chow and C. Saint, *Chem. Eng. J*., **15**, 49 (2009).
42. D. F. Ollis, E. Pelizzatti and N. Serpone, *Environ. Sci. Techno*., **35**, 1523 (1991).
43. K. Mehrota, G. S. Yablonsky and A. K. Ray, *Chemosphere*, **60**, 1427 (2005).
44. M. L. Chin, A. R. Mohamed and S. Bhatia, *Chemosphere*, **57**, 547 (2004).
45. X. L. Zhu, C. W. Yuan, Y. C. Bao, J. H. Yang and Y. Z. Wu, *J. Mol. Catal. A: Chem*., **229**, 95 (2005).
46. W. Y. Wang, A. Irawan and Y. Ku, *Wat. Res*., **42**, 4725 (2008).
47. A. P. Toor, A. Verma, C. K. Jotshi, P. K. Bajpai and V. Singh, *Dye Pigment*, **68**, 53 (2006).
48. A. N. Okte and O. Yilmaz, *Appl. Catal. B: Environ*., **85**, 92 (2008).
49. J. H. Sun, Y. K. Wang, R. X. Sun and S. Y. Dong, *Mater. Chem. Phys*., **115**, 303 (2009).
50. M. Muruganandham and M. Swaminathan, *J. Hazard. Mater*., **B135**, 78 (2006).
51. N. San, A. Hatipoglu, G. Kocturk and Z. Cinar, *J. Photochem. Photobio. A: Chem*., **146**, 189 (2002).
52. M. Sleiman, D. Vildozo, C. Ferronato and J. M. Chovelon, *Appl. Catal. B: Environ*., **77**, 1 (2007).
53. C. M. So, M. Y. Cheng, J. C. Yu and P. K. Wong, *Chemosphere*, **46**, 905 (2002).
54. Y. H. Ao, J. J. Xu, D. G. Fu, X. W. Shen and C. W. Yuan, *Colloids Surf. A: Physicochem. Eng. Aspects*, **312**, 125 (2008).